Three-photon absorption in Nd-doped yttrium aluminum garnet

Mark A. Kramer and Robert W. Boyd
Institute of Optics, University of Rochester, Rochester, New York 14627
(Received 12 September 1980)

Resonantly enhanced, three-photon absorption has been observed in Nd-doped yttrium aluminum garnet (Nd:YAG). This process probes the energy-level structure of the Nd $4f^25d^1$ electron configuration. The measured maximum value of the three-photon absorption cross section is $\sigma^{(3)} = 1 \times 10^{-81}$ cm^6 s^2/photon^2, which is in good agreement with the expected size of the effect.

I. INTRODUCTION

This paper presents the results of a study of resonantly enhanced, three-photon absorption in Nd-doped yttrium aluminum garnet ($Y_3Al_5O_{12}$) or Nd:YAG. The trivalent ions of the rare-earth elements, such as Nd^{3+}, are characterized by energy levels which remain relatively sharp even in a crystalline environment, and thus crystalline solids doped with rare-earth ions present interesting systems in which to study resonantly enhanced optical nonlinearities. While a number of different types of optical nonlinearity can be studied in impurity-doped crystals, such as two-photon absorption,[1,2] saturated absorption,[3] degenerate four-wave mixing,[4,5] and polarization spectroscopy,[6] this paper focuses on the process of three-photon absorption. Through the absorption of three visible photons we are able to excite Nd^{3+} energy levels which lie approximately 40 000 to 70 000 cm^{-1} above the ground state, and hence belong to the $4f^25d^1$ electron configuration. Since Nd:YAG is essentially opaque for radiation of wave numbers greater than 42 000 cm^{-1}, the technique of three-photon absorption allows us to probe regions of the $4f^25d^1$ configuration which are inaccessible using one-photon techniques.

II. LINEAR SPECTROSCOPY OF Nd:YAG

Some of the single-photon spectroscopic properties of Nd:YAG that are needed for the interpretation of the three-photon-absorption results are presented here. An absorption spectrum of our 1 wt.%, Nd:YAG taken on a Carey model 14 recording spectrophotometer is shown in Fig. 1. The numerous sharp absorption features in the range 2500 to 9000 Å are due to the Nd^{3+} ion. Since the fundamental absorption edge of YAG occurs[7] at 1920 Å, the observed 2400 Å cutoff wavelength in Nd:YAG has been interpreted by Krupke[8] as due to a distortion of the host lattice by the Nd dopant.

Figure 2 shows an energy-level diagram of Nd:YAG which combines our results of Fig. 1 with previously published data. The region between 0 and 70 000 cm^{-1} contains a large number of energy levels belonging to the $4f^3$ electron configuration. Since the $4f$ electrons are shielded from the crystalline electrostatic field by the closed outlying $5s$ and $5p$ shells, energy levels in this region are very narrow. For energies below 21 000 cm^{-1}, we have plotted the energy levels determined by Koningstein and Geusic[9] including their level identifications. For energies in the range 27 000 and 40 000 cm^{-1}, we have plotted

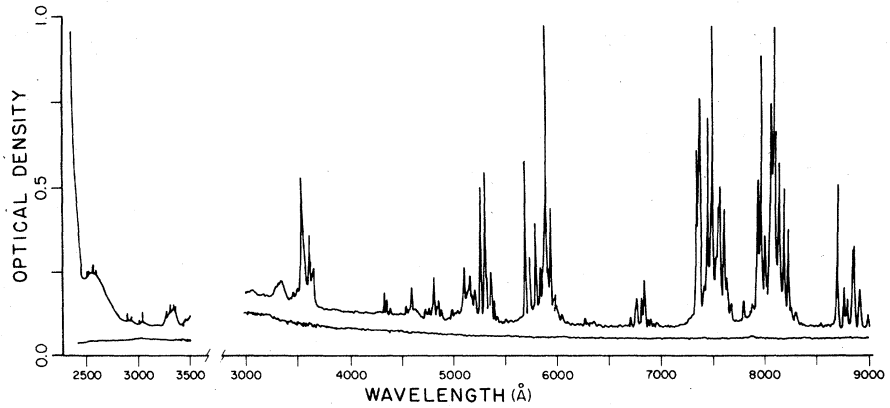

FIG. 1. Absorption spectrum of 0.5-cm Nd:YAG crystal at 300 K.

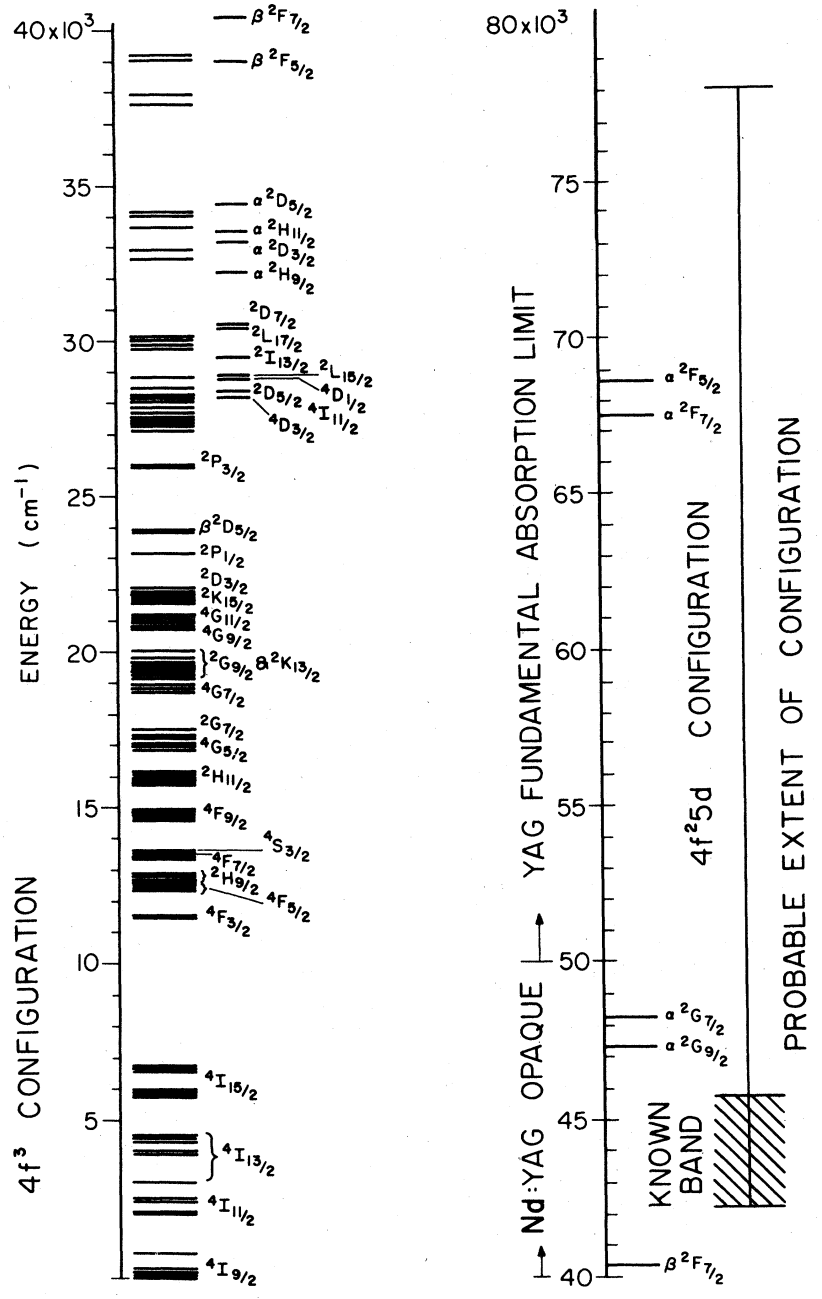

FIG. 2. Nd:YAG energy-level diagram.

the energy levels inferred from our data of Fig. 1 along side the identified energy levels predicted by a calculation described by Koningstein.[10] The agreement between measured and predicted energies becomes worse at higher energy. Several additional predicted energy levels at energies greater than 40 000 cm^{-1} are also plotted.

The excited $4f^25d^1$ electron configuration produces broad spectral features, believed to lie 40 000 to 80 000 cm^{-1} above the ground state, since the $5d$ electron is not shielded from the crystal field. Weber[11] has determined that one band belonging to this configuration extends from 43 000 to 46 000 cm^{-1}. In different host crystals, additional bands are found whose positions are somewhat host dependent,[12] but these bands have not previously been well studied in Nd:YAG because of the lack of transparency of YAG in this region.

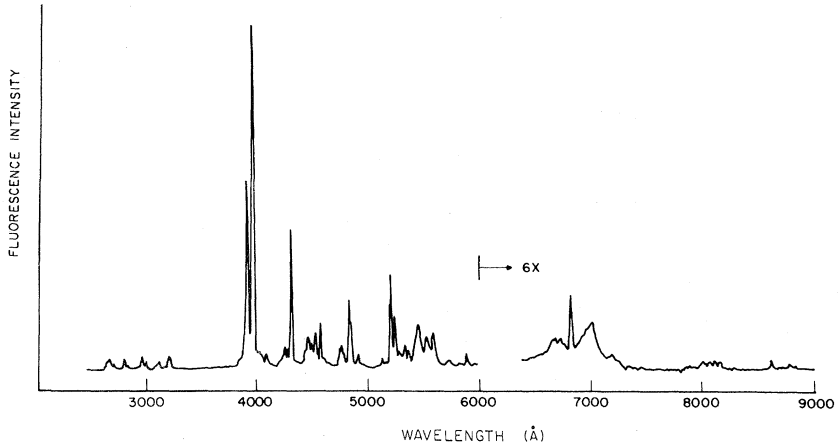

FIG. 3. Spectrum of the emission excited by three-photon absorption at an excitation wavelength of 5935 Å.

III. MEASUREMENT OF THREE-PHOTON ABSORPTION

Our experimental method of studying three-photon absorption involves monitoring the fluorescence excited by a 6-ns pulse of 50-kW maximum peak power from a Molectron nitrogen-laser-pumped dye laser. Most of the spectral interval between 4300 and 6600 Å is accessible through the use of the laser dyes coumarin 2, coumarin 4, fluorescein, rhodamin 6*G*, rhodamin *B*, and cresyl violet perchlorate. The dye laser beam is focused to a spot size $w_0 = 13$ μm (w_0 is the beam radius at the $1/e^2$ intensity points) in a 5-mm-long sample of 1-wt.% Nd:YAG. When the dye laser is tuned to certain wavelengths throughout the 4300–6500-Å region, fluorescence of blue color is emitted by the focal volume and is of sufficient intensity to be readily observed by eye.

The emission spectrum of this fluorscence has been measured using a 0.25-m monochromator and an EMI 9558Q photomultiplier. The emission spectrum following excitation at 5935 Å is shown in Fig. 3; the emission spectrum is virtually unchanged for excitation at other wavelengths. If the laser is defocused the emission at wavelengths shorter than the laser wavelength disappears, whereas the longer-wavelength features are nearly unchanged, thus implying that the shorter-wavelength features are due to a nonlinear optical process.

All of the emission features at wavelengths shorter than the excitation wavelength have a decay time of $3 \pm \frac{1}{2}$ μs, thus suggesting that they have the same upper level, and in fact the wavelengths of these features are consistent with decay from the $\beta^2 F_{5/2}$ level to lower states. The features between 8000 and 9000 Å, which can be excited through linear absorption, originate at the $^4F_{3/2}$ level and have a measured decay time of 250 ± 25 μs, in agreement with other measurements.[8] The broad emission feature of decay time 1 ms near 6900 Å has the same line shape as that measured by Taylor[13] for Cr in YAG. Since in addition the excitation spectrum of this feature is inversely correlated with the Nd absorption spectrum, we conclude that the 6900-Å feature is due to a Cr impurity in our sample.

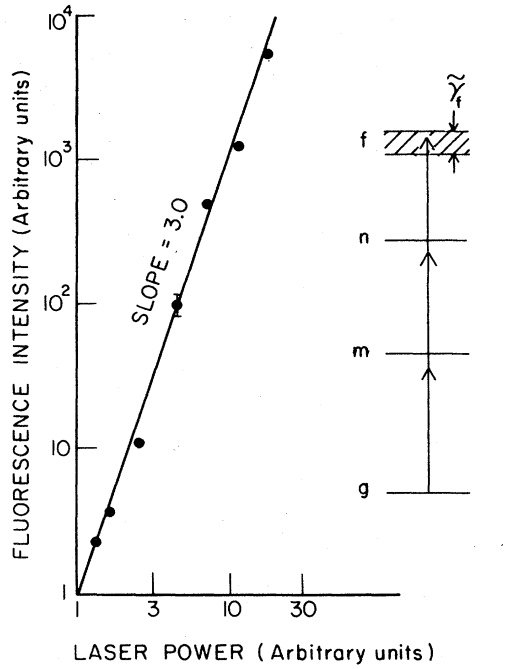

FIG. 4. Laser-power dependence of the emission lines near 4000 Å. The cubic power dependence suggests the excitation process shown in the inset, in which an ion makes a transition from level g to level f of breadth $\tilde{\gamma}_f$ by the simultaneous absorption of three photons of energy $\tilde{\nu}$. Levels m and n are intermediate states.

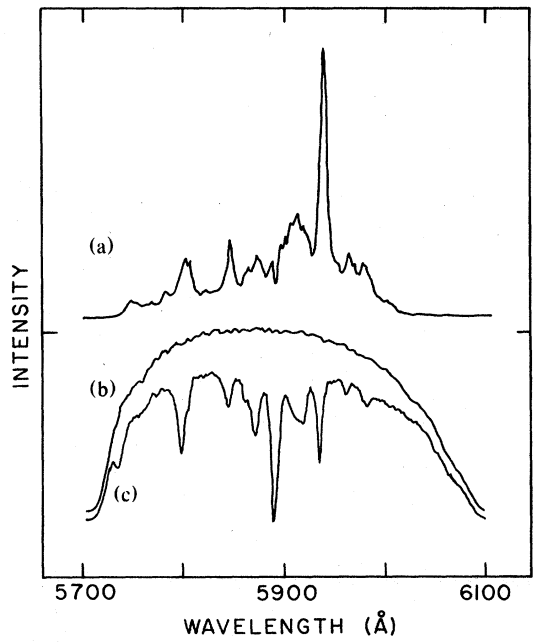

FIG. 5. (a) Excitation spectrum of 4000-Å emission lines. (b) Output power vs wavelength of the dye laser using rhodamine 6G. (c) Laser power transmitted by the 5-mm-long crystal.

In order to determine the excitation process giving rise to the short-wavelength emission, we have measured the laser-power dependence of the strong emission features near 4000 Å with the laser tuned to 5935 Å. A cubic dependence on laser power is found as shown in Fig. 4, thus suggesting that the excitation process is three-photon absorption to the $4f^25d^1$ configuration followed by a nonradiative decay to the fluorescing $^2F_{5/2}$ level of the $4f^3$ configuration.

We have studied the intensity of the 4000-Å features as a function of excitation wavelength over much of the visible spectrum. Typical data are shown in Fig. 5 using Rhodamine 6G in the dye laser. Curve (a) gives the excitation spectrum for the 4000-Å emission, curve (b) gives the output spectrum of the dye laser, and curve (c) shows the laser power transmitted by the 5-mm-long crystal. Each peak in the excitation spectrum a corresponds to an absorption maximum in curve (c), thus indicating that the three-photon absorption process is resonantly enhanced when the excitation wavelength is resonant with a one-photon transition. Figure 6 shows the resonances that we have found in the nonlinear excitation spectrum of the 4000-Å features. Most of these features can be understood in terms of single-photon resonances. The interpretation of these features will be discussed further in the conclusions.

IV. MEASUREMENT OF THE THREE-PHOTON CROSS SECTION

We have made an approximate measurement of the cross section for three-photon absorption for excitation at the vacuum wavelength $\lambda = 5935$ Å, which corresponds to the largest peak in the excitation spectrum of Fig. 5. The three-photon-absorption cross section $\sigma^{(3)}$ is defined such that the induced transition rate per ion is given by $\sigma^{(3)}I^3$, where the laser intensity I is given in units of photons/cm^2 s. For the purposes of this measurement, we assume that the quantum yield for fluorescence from the $\beta^2F_{5/2}$ level following excitation by three-photon absorption is equal to 0.21, the ratio of the measured fluorescent decay time to the 14-μs radiative lifetime of the $\beta^2F_{5/2}$ level calculated from the Judd[14]-Ofelt[15] theory. By measuring the intensity of the emission features near 4000 Å with a calibrated photomultiplier, we have determined that, at maximum laser power, a total number $N = 2\times10^{10}$ photons are emitted from this level for each laser pulse. The three-photon cross section can be related to N and to the known properties of the laser beam through the relation

$$N = \eta T \int \rho\sigma^{(3)} I(r,dz)^3 2\pi r\, dr\, dz \ , \qquad (1)$$

where $T = 5$ ns is the equivalent duration of the laser pusle, $\rho = 1\times10^{20}$ cm^{-3} is the Nd number density,

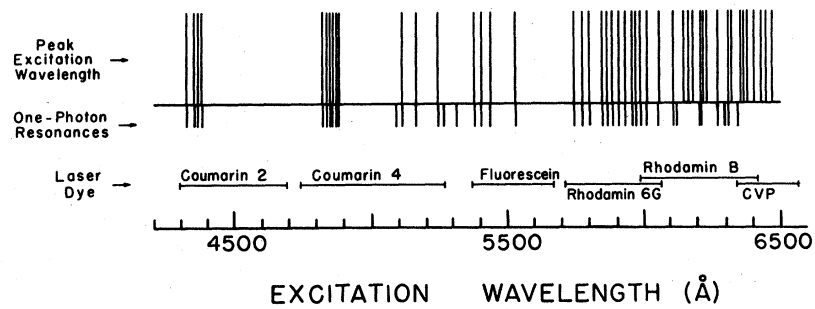

FIG. 6. Excitation wavelengths of the fluorescence induced by three-photon absorption. One-photon resonances and laser tuning ranges are also indicated.

and where the laser intensity $I(r,z)$ varies with the cylindrical polar coordinates r and z as[16]

$$I(r,z)=\frac{P}{\frac{1}{2}\pi w(z)^2}e^{-2r^2/w(z)^2} \quad . \tag{2}$$

Here P is the power in the laser beam and the functional form of the "beam radius" $w(z)$ is given by

$$w(z)^2=w_0^2\left[1+\frac{\lambda z}{n\pi w_0^2}\right] \quad , \tag{3}$$

w_0 being the minimum value of $w(z)$ which it attains at the beam waist, and n being the refractive index of the host. The limits of integration on Eq. (1) strictly correspond to the volume of the crystal, but for our experimental conditions the focal volume and thus the volume giving rise to appreciable fluorescence was confined to a small region interior to the crystal, and thus the limits of integration on Eq. (1) may be allowed to approach infinity. If the variation in laser power due to absorption is assumed negligible over the longitudinal extent of the focal region, the laser power P may be held constant in performing the integration in Eq. (1), leading to a closed-form expression for the three-photon cross section:

$$\sigma^{(3)}=\frac{3w_0^2(\lambda/n)N}{2TP^3\eta} \quad . \tag{4}$$

This expression can be evaluated numerically assuming a peak laser power at the focus of 30 kW or 1×10^{23} photon/s to give the value $\sigma^{(3)}=1\times10^{-80}$ cm^6 s^2/photon^2. Owing to uncertainties in the intensity of the laser beam and the calibration of the photomultiplier, this measured cross section is not certain to better than a factor of 10. The other resonances which we have observed have cross sections smaller than this maximum value by factors of 3 to 100.

V. THEORETICAL INTERPRETATION

Many of the experimental results presented here can be understood in terms of a simple theoretical argument based on third-order, time-dependent, quantum-mechanical perturbation theory. We can define as before a three-photon-absorption cross section $\sigma^{(3)}$ such that the three-photon transition rate per atom is given by $\sigma^{(3)}I^3$, where I is the laser intensity in units of photons/cm^2 s. The quantum-mechanical predictions of the three photon cross section is given by

$$\sigma^{(3)}=\frac{4\pi^2\tilde{\nu}^3}{\hbar^3c^5}\left[\frac{E_{\rm loc}}{E}\right]^6\left|\sum_{nm}\frac{\mu_{fm}\mu_{mn}\mu_{ng}}{(\tilde{\nu}_{ng}-2\tilde{\nu}-i\tilde{\gamma}_n/2)(\tilde{\nu}_{mg}-\tilde{\nu}-i\tilde{\gamma}_m/2)}\right|^2\left[\frac{\tilde{\gamma}_f/2\pi}{(\tilde{\nu}_{fg}-3\tilde{\nu})^2+(\tilde{\gamma}_f/2)^2}\right] \quad , \tag{5}$$

where all antiresonant contributions to the cross section, resulting from negative frequency components in the applied laser field, are ignored. Here $(E_{\rm loc}/E)=\frac{1}{3}(n^2+2)$ is a local-field correction,[17] $\tilde{\nu}$ is the laser wave number, $\hbar$ is Planck's constant divided by 2π, c is the speed of light in vacuum, μ_{ij} is the electric dipole matrix element connecting levels i and j, $\tilde{\nu}_{ng}$ is the energy of level n with respect to the ground level g in units of wave numbers, and $\tilde{\gamma}_i$ is the full width at half maximum (FWHM) breadth in wave numbers of the energy level i, which is assumed to have a Lorentzian probability distribution. This nomenclature is illustrated in the inset of Fig. 4. Equation (5) is derived by calculating to third order in time-dependent perturbation theory the probability amplitude for the ion to be in state f at time t and hence determining a transition probability per unit time using Fermi's golden rule.[18] Damping is introduced phenomenologically to give rise to the $i\gamma$'s in the resonance denominators.

Equation (5) predicts a resonance in the three-photon cross section whenever the laser becomes resonant with a one- or two-photon allowed transition, and requires an energy-conserving final state, located at an energy $3\tilde{\nu}$ above the ground state. If all of the matrix elements appearing in Eq. (5) were known, the double summation in this equation could be evaluated, allowing a quantitative comparison of theory with experiment. While the matrix elements connecting the lower levels of the $4f^3$ configuration can be evaluated using the Judd[14]-Ofelt[15] theory and the known intensity parameters[8] for YAG, the matrix elements connecting $4f^3$ levels with the $4f^25d^1$ levels are not known, and the Judd-Ofelt theory cannot be applied to the calculation of matrix elements involving levels of the $4f^3$ configuration that are near the $4f^25d^1$ levels. An order of magnitude estimate of the size of the three-photon cross section can be made, however, by assuming that only a single level n and a single other level m contribute appreciably to $\sigma^{(3)}$ so that the double summation reduces to a single term. Equation (5) can then be evaluated by assuming the following parameters: $\tilde{\nu}=17\,000$ cm^{-1}; $n=1.8$; $|\mu_{ng}|=|\mu_{mn}|=2\times10^{-20}$ esu, typical of intraconfiguration crystal-field transition moments, $\mu_{fm}=10^{-18}$ esu, typical of interconfiguration transition moments; $|\tilde{\nu}_{mg}-\tilde{\nu}|<\tilde{\gamma}_m$, $|\tilde{\nu}_{ng}-2\tilde{\nu}|<\tilde{\gamma}n$, and $|\tilde{\nu}_{fg}-3\tilde{\nu}|<\tilde{\gamma}_f$, corresponding to a laser tuned nearly to a one-, two-, and three-photon resonance; $\tilde{\nu}_n=\tilde{\nu}_m=20$ cm^{-1}, a typical $4f^3$ line breadth; and

$\tilde{\gamma}_f = 5000$ cm^{-1}, a typical breadth of a $4f^25d^1$ band, leading to a predicted cross section of $\sigma^{(3)} = 3 \times 10^{-80}$ cm^6 s^2/photon^2. This theoretical cross section, estimated using the most optimistic choice of parameters, is comparable to the maximum measured cross section of 1×10^{-80} cm^6 s^2/photon^2.

The theory developed here treats the excitation process as one involving the simultaneous absorption of three laser photons. If however the excitation wavelength corresponds to a one-photon resonance, the excitation process can entail linear absorption to a real level followed at some later time by the absorption of two additional photons. In principle, these processes differ in that the former is a coherent process whereas the latter need not be, although both processes lead in lowest order to a transition rate proportional to the third power of the laser intensity with a cross section given by Eq. (5). For the case in which a real level is excited, it is possible that some nonradiative relaxation occurs before the additional absorption completes the excitation process, as has been suggested by Singh and Geusic[19] in their discussion of the excitation of visible fluorescence in several rare-earth compounds using a wavelength of 1.06 μm.

VI. CONCLUSIONS

We have observed the fluorescent decay following resonantly enhanced three-photon absorption in Nd:YAG. The maximum measured cross section for three-photon absorption, occurring for an excitation wavelength of 5935 Å, is equal to 1.3×10^{-80} cm^{6}s^2/photon^2. This excitation wavelength is nearly one-photon resonant with the $^4G_{5/2}$ level and two-photon resonant with an unidentified level 33 700 cm^{-1} above the ground state. The theoretical model presented in the text gives a calculated value for the case of one- and two-photon resonance of 3.0×10^{-80} cm^6 s^2/photon^2, in good agreement with the measured value.

The peak excitation wavelengths for fluorescence excited by three-photon absorption have been determined for much of the visible spectrum and are shown in Fig. 6. Most of these excitation features are known to be enhanced by one-photon resonances. The additional features are perhaps one- or two-photon enhanced by energy levels which do not lead to dominant linear absorption lines and hence do not appear in the energy-level diagram of Fig. 2, or perhaps these additional features are due to three-photon absorption to a final state belonging to the $4f^3$ configuration, such as the $\alpha^2G_{7/2}$ or $\alpha^2G_{9/2}$ level.

From the spectrum of three-photon absorption shown in Fig. 6, we are also able to ascertain the approximate positions of energy bands belonging to the $4f^25d^1$ configuration, even though these energies lie above the YAG absorption edge. Our technique does not rule out other possible energy levels, but does determine the existence of energy levels in the ranges 46 000–52 000, 54 000–59 000, 61 000–62 500, and 68 000–70 000 cm^{-1} above the ground state.

ACKNOWLEDGMENTS

The authors are grateful to D. L. Dexter, M. J. Stavola, W. Krupke, and L. G. DeShazer for useful discussions and to M. L. Weber for providing us with some unpublished matrix elements of Nd^{3+}. The samples used in this work were provided by the University of Rochester's Laboratory for Laser Energetics. This work was partially supported by NSF Grant No. SER77-06914 and No. ENG79-08038.

[1]W. Kaiser and C. G. B. Garrett, Phys. Rev. Lett. 7, 229 (1961).
[2]U. Fritzler and G. Schaack, J. Phys. C 9, L23 (1976).
[3]R. K. Ahrenkeil, J. F. Figueira, C. R. Phipps, Jr., D. J. Dunlavy, S. J. Thomas, and A. J. Sievers, Appl. Phys. Lett. 33, 705 (1978).
[4]D. C. Hamilton, D. Heiman, J. Feinberg, and R. W. Hellwarth, Opt. Lett. 4, 125 (1979).
[5]D. E. Watkins, J. F. Figueira, and S. J. Thomas, Opt. Lett. 5, 169 (1980).
[6]J. H. Lee, J. J. Song, M. A. F. Scarparo, and M. D. Levenson, Opt. Lett. 5, 196 (1980).
[7]G. A. Slack, D. W. Oliver, R. M. Chrenko, and S. Roberts, Phys. Rev. 177, 1308 (1969).
[8]W. F. Krupke, IEEE J. Quantum Electron. 7, 153 (1971).
[9]J. A. Koningstein and J. E. Geusic, Phys. Rev. 136, A711 (1964).
[10]J. A. Koningstein, J. Chem. Phys. 44, 3957 (1966).
[11]M. J. Weber, Solid State Commun. 12, 741 (1973).
[12]K. H. Yang and J. A. DeLuca, Phys. Rev. B 17, 4246 (1978).
[13]M. J. Taylor, Proc. Phys. Soc. London 90, 487 (1967).
[14]B. R. Judd, Phys. Rev. 127, 750 (1962).
[15]G. S. Ofelt, J. Chem. Phys. 37, 511 (1962).
[16]H. Kogelnik and T. Li, Appl. Opt. 5, 1550 (1966).
[17]W. B. Fowler, in *Physics of Color Centers*, edited by W. B. Fowler (Academic, New York, 1968), p. 64.
[18]L. I. Schiff, *Quantum Mechanics*, 3rd ed. (McGraw-Hill, New York, 1968), Sec. 35.
[19]S. Singh and J. E. Geusic, in *Optical Properties of Ions in Crystals*, edited by H. M. Crosswhite and H. W. Moos (Interscience, New York, 1967).